Int. J. Econ. Environ. Geol. Vol. 11 (1) 72-76, 2020

Journal home page: www.econ-environ-geol.org

Open Access

ISSN: 2223-957X

Dehydroxylation of Minerals of Gadisunkapur Area with Special Reference to FTIR and Thermal Study

Marularadhya C. Hiremath[1]*; A. Sreenivasa[2]

[1, 2]Department of Studies in Geology, Karnatak University, Dharwad, Karnataka-580003

*Email: siddhu.hiremath8@gmail.com

Received: *03 August, 2019* ***Accepted: 17*** *February, 2020*

Abstract: This paper attempts to explain the presence of OH group for micas along with some sulfate, chlorite, quartz and feldspar minerals. These minerals are found to be associated with barite vein, metasediments (quartz-chlorite schist), metarhyolite and varieties of granitic rocks of Gadisunkapur area of Hungund-Kushtagi Schist belt. The samples were collected in and around Gadisunkapur village of Bagalkote district, Karnataka and further processed to determine OH group anion in different minerals present based on FTIR and Thermal studies such as Thermogravimetric analysis (TGA) and Differential Thermal analysis (DTA). The high temperature dehydroxylation is investigated using this analysis. Furthermore, present study indicates the presence of different extra species (CO_2, CO_3^{2-} and OH^-). The results show the incorporation of CO_2 into the structures due to heating or enhanced by the dehydroxylation process.

Keywords: FTIR, TGA, DTA, OH group, Gadisunkapur, Hungund-Kushtagi schist belt.

Introduction

Gadisunkapur area has some barite traces, barite occurrence in the study area rocks are having mica, feldspar, chlorite and quartz minerals. Biotite and muscovite are the dominant phyllosilicates observed in the lithounits of the study area. Fourier Transform Infrared Spectroscopy (FTIR) and Thermal study carried out in the study area shows the presence of OH molecules. The shape of micas is primarily based on interconnected six member rings of SiO^{4-} tetrahedra that make bigger in endless sheets. Three out of 4 oxygen’s from each tetrahedron are shared with different tetrahedra. This ends in a simple structural unit of $Si2O^{-2}$. FTIR and thermal studies play a prominent role in identifying the minerals present in the rock samples of the study area. In geology, natural micas release cation when subjected to weathering and hydrothermal alterations (Kapoor et al., 1981; Taylor et al., 2000). The thermal study and FTIR carried out gives the detailed spectral changes related to different vibrational bands (e.g. these of O- H, Si-O, Al-O vibrations) and is compared with IR data.

Geological setting

The Hungund-Kushtagi schist belt is having a general trend of NW-SE that is exposed inside the northwestern a part of Eastern Dharwar Craton (EDC). Geologically, the belt mainly includes mafic volcanic rocks with subordinate felsic volcanic rocks and metasediments (quartz-chlorite schist, banded iron formation, meta argillite and greywacke) Bhat et al (1996). According to Naqvi et al., (2006) said geochemically volcanic rocks are high Mg, high Fe, and excessive Mg-Fe basalts, high Mg-dacites, andesites and adakites. A form of granitoids is exposed inside the adjoining place of the greenstone belt (Dey et al. 2003, 2009, 2012; Dey, 2006, 2011; Mohan et al, 2013).

Rocks of Hungund-Kushtagi schist belt are divided into Ilkal and Muddenur formations. The study area falls in contact zone of Ilkal and Muddenur formations and composed of amphibolites, metabasalts, metasediments (quartz, chlorite-schist), metarhyolite and varieties of granites. In the study area few barite veins are also reported which are associated with metabasalts, metasediments and granites. The amphibolite of the study area occurs as lensoid bodies which are reported in the northeastern area of Gadisunkapur village adjacent to Ilkal halla. The granites pink and grey variants are seen in western part of Gadisunkapur village, along Raichur-Bachi state highway. These granites show porphyritic texture. Barite occurs in vein forms varying from 2-4meter in width and 10-20meters length within metasediments (quartz-chlorite- schist) and rarely traces are found in granites. Metarhyolite is observed in the western and north eastern part of Jammaldinni village which shows aphanitic texture with varying colour from light green to reddish brown (Marualradhya et al, 2019).

Materials and Methods

Fourier transform infrared (FTIR) spectroscopy is an alternative technique for acquiring quantitative mineralogy. The mineralogy of a combination may be extracted from its FTIR spectrum because minerals show most of the fundamental vibration modes in the mid-infrared region 4000cm^{-1} to 400cm^{-1}. Infrared spectra of minerals of Gadisunkapur area were carried out using Carl Zeiss UR-10 and X-99 IR spectrometer with the help of mull media method. The collected samples were finely powdered into 150# size then small quantity of powdered samples was taken in agate mortar and powdered to attain size of talcum powder. This powder is mixed with pure paraffin oil forming a suspension of minute crystallites in a viscous medium. Furthermore, skinny plate is prepared through squeezing and (of both Nacl or KBr) plate of resultant received paste (Mahesh et al, 2014).

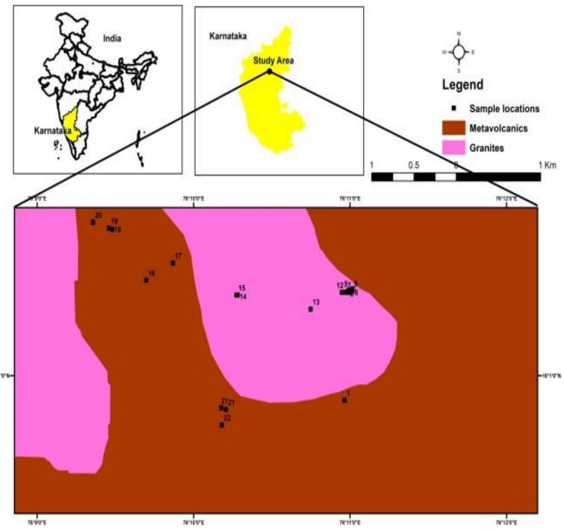

Fig. 1 Geological map of the study area

Thermogravimetric evaluation is a way in which weight reduction of substance is studied while it is subjected to controlled temperature. TGA approach performs an essential function in finding distinct minerals in geology. Many times TGA curve resembles to the DTA curve of the mineral. When powdered sample is subjected to heating up to the temperature 1400^{O} C, it loses its weight for a period of 15minutes. A 0.5gm of powder has been taken and the weight reduction of substance is calculated and plotted in graph (Rajendra et al, 2018).

Differential thermal evaluation (DTA) is a method wherein the temperature distinction between a substance and a reference material is measured as a characteristic of temperature, while the substance and reference materials are subjected to the same controlled temperature. DTA requires reference fabric, which is referred to as substance. It is usually thermally inactive over the temperature variety. The crucial character of the reference material is its thermal traits and the particle length. DTA method could be very beneficial in identifying minerals, which goes through transformation which is heated to controlled temperature beneath 1400^{o}C (Rajendra et al., 2018).

DTA technique is useful in both qualitative and semi-qualitative studies, which liberates or absorbs energy when subjected to heating and results in transformations such as dehydration, oxidation, decomposition, phase changes and dehydroxylation (Rajendra et al, 2018).

Results and Discussion

The bands between the range 3400cm^{-1} to 3700cm^{-1} with stretching vibration of V(OH) indicate the presence of OH molecule for chlorite mineral. The OH deformation of water for specific clay minerals is determined in the range of 1612cm^{-1} to 2336cm^{-1} (Saikia et al., 2010). The peaks at 3782cm^{-1} and 3684cm^{-1} are assigned V(OH) vibration of OH molecule which suggests the presence of biotite. A stretching vibration for biotite of adsorbed water V(H_2O) is found at 3374cm^{-1}. Further the sturdy band around 1595cm^{-1} shows the presence of adsorbed water of OH for biotite. The untreated sample did not incorporate CO_3^{2-} and CO_2 species due to lack of their characteristic absorption indicators at 1400cm^{-1} and close to 2345cm^{-1}. The structurally incorporated hydroxyl groups in mica show O-H stretching bands around 3626cm^{-1}, 3702cm^{-1} and 3590cm^{-1} (Ming Zhang et al., 2005). The bands around 3414cm^{-1} show V (H2 O) (Adsorbed water) for micas. Furthermore, the strong bands around 1595cm^{-1} are assigned to δ(H2 O)(adsorbed water) which suggest the presence of mica.

The differential thermal analysis noted from 932^{o} to 1169^{o} C shows dehydroxylation of biotite, which is endothermic in nature where water loss is observed as a result of internal arrangement of the atoms.

Weight loss of 0.084% to 0.936 from the temperature 168.61^{o} to 394.67^{o} is attributed to dehydroxylation of muscovite. During the dehydroxylation of muscovite, structural transformation of layer silicates were reported (Muller et al, 2000). In muscovite, the O–H vector does no longer point directly in the direction of the interlayer cation, instead the proton is close to the interlayer cation, K, and a bonded oxygen [K–O(2)] of the basal oxygen-atom plane. The K-O(2) bond distance is longest at room temperature and therefore is considered as weakest (Guggenheim et al, 1987). At high temperatures studied, this bond remains longer and increases in length at rapid rate than the other K-O bonds. The closeness of the proton to the K-O(2) bond and the rate at which this bond weakens at high temperatures suggests the way for dehydroxylation (Annibale et al., 2002). Weight loss of 0.050% to 0.423% from the temperature 432.02^{o} C to 688.66^{o}C is attributed to dehydroxylation of quartz admixture of magnetite, olivine and spinel. The total mass loss of the sample is due to liberation of adsorbed water and hydroxyl group from the lattice structure which corresponds to the formation of new phases like α↔β quartz inversion at temperature around 500^{o}C and Si-Al spinel formation at temperature 650^{o}C (Escalera et al, 2012). Weight loss of 0.275% to 3.338% from the temperature 1027.13^{o}C to 1169.09^{o}C is attributed to dehydroxylation of cristoballite leading to formation of mullite which depends on potassium and iron contents in the samples (Fig. 5.9-5.16).

Table 1 Bands in the infrared spectrum of minerals

S.No	Sample No	Frequency in Cm-1	Tentative assignment	Mineral identified
1	S-4	3702.70w	V(OH)	Chlorite
		3414.05b	V(H2O) (Adsorbed water)	Biotite
		1595.09s	δ(H2O) (adsorbed water)	Biotite
2	S-7	3735.08w	V(OH)	Biotite
		3702.70w	V(OH)	Chlorite
		3626.17lsh	V(OH)	Chlorite
		3590.84lsh	V(OH)	Biotite
		3413.15b	V(H_2O) (Adsorbed water)	Biotite
		1595.09s	δ(H_2O) (adsorbed water)	Biotite
3	S-10	3732.13w	V(OH)	Biotite
		3702.70w	V(OH)	Chlorite
		3629.11w	V(OH)	Chlorite
		3415.35b	V(H_2O) (Adsorbed water)	Biotite
4	S-11	3767.46w	V(OH)	Biotite
		3649.71w	V(OH)	Muscovite
		3614.39sh	V(OH)	Muscovite
		3418.61b	V(H_2O)	Muscovite
5	S-17	3732.13w	V(OH)	Biotite
		3696.81w	V(OH)	Biotite
		3375.78b	V(H_2O) (Adsorbed water)	Biotite
6	S-19	3735.08w	V(OH)	Biotite
		3619.21w	V(OH)	Muscovite
		3402.45b	V(H_2O) (adsorbed water)	Biotite
7	S-21	3732.13w	V(OH)	Biotite
		3699.75w	V(OH)	Biotite
		3624.35s	V(OH)	Muscovite
		3373.86b	V(H_2O) (adsorbed water)	Biotite

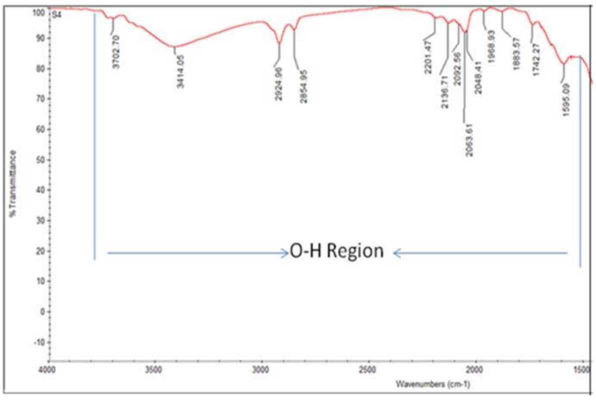

Fig. 1 Infrared spectra of sample

Thermal analysis was carried out employing TGA-DTA (Make SDT Q600 V20.9 TA). In the present study 8 samples were subjected to TGA and DTA analyses. Furthermore, a brief description about sample number, name, type of reaction and minerals identified are tabulated in Tables 2 & 3.

Table 2: Results of differential analysis of (DTA) of barite of Gadisunkapur area (after Marularadhya and Sreenivasal, 2019)

S.No	Sample name	Endothermic peak	Mineral identified	Type of Reaction
1	S-4	1162.22^{o}-1167.72^{o}C	Biotite	Dehydroxylation
2	S-7	1163.47^{o}-1169.99^{o}C	Biotite	Dehydroxylation
3	S-10	1162.25^{o}-1167.29^{o}C	Biotite	Dehydroxylation
4	S-11	1151.64^{o}-1157.55^{o}C	Biotite	Dehydroxylation
5	S-17	1101.11^{o}-1141.44^{o}C	Biotite	Dehydroxylation
6	S-19	1107.36^{o}-1129.61^{o}C	Biotite	Dehydroxylation
7	S-21	932.07^{o}-1008.02^{o}C	Biotite	Dehydroxylation
8	S-23	1084.70^{o}-1147.00^{o}C	Biotite	Dehydroxylation

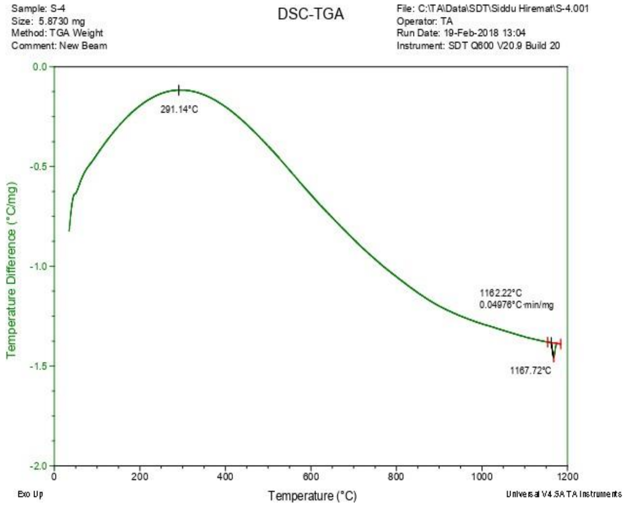

Fig. 2 DTA graph of sample

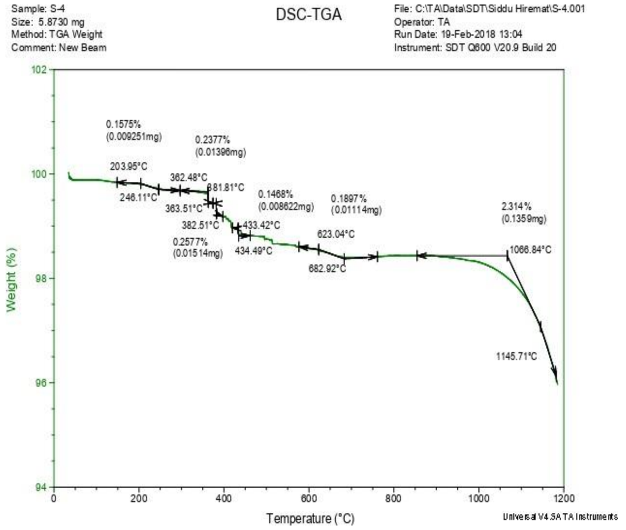

Acknowledgement

I would like to thank Chairman, Dept. of Studies in Geology, Karnatak University for providing all necessary help. First author would like to thank, funding agency DST PURSE PHASE-II (Department

Table 3 Results of thermo-gravimetric- analysis (TGA) of barite of Gadisunkapur area (after Marularadhya, and Sreenivasa, 2019)

S.No	Sample	Weight loss %	Temperature	Mineral Identified	Type of reaction
1	S-4	0.1575	203.95°-246.11°C	Muscovite	Dehydroxylation
		0.2377	362.48°-363.51°C	Muscovite	Dehydroxylation
		0.2577	381.81°-382.51°C	Muscovite	Dehydroxylation
		0.1468	433.42°-434.49°C	Quartz admixture of magnetite, olivine and spinel	Dehydroxylation
		0.1897	623.04°-682.92°C	Quartz admixture of magnetite, olivine and spinel	Dehydroxylation
		2.314	1066.84°-1145.71°C	Cristoballite	Dehydroxylation
2	S-7	0.2530	168.61°-278.49°C	Muscovite	Dehydroxylation
		0.1286	432.02°-433.06°	Quartz admixture of magnetite, olivine and spinel	Dehydroxylation
		0.0988	490.05°-490.34°C	Quartz admixture of magnetite, olivine and spinel	Dehydroxylation
		0.1984	624.75°-625.93°C	Quartz admixture of magnetite, olivine and spinel	Dehydroxylation
		0.0501	686.17°-688.66°C	Quartz admixture of magnetite, olivine and spinel	Dehydroxylation
		1.964	1027.13°-1127.63°C	Cristobalite	Dehydroxylation
3	S-10	0.333	201.67°-243.42°C	Muscovite	Dehydroxylation
		0.225	384.70°-385.22°C	Muscovite	Dehydroxylation
		0.081	456.49°-457.23°C	Quartz admixture of magnetite, olivine and spinel	Dehydroxylation
		0.153	604.58°-663.22°C	Quartz admixture of magnetite, olivine and spinel	Dehydroxylation
		1.863	1037.35°-1131.07°C	Cristobalite	Dehydroxylation
4	S-11	0.554	393.70°-394.67°C	Muscovite	Dehydroxylation
		3.338	1144.65°-1169.09°C	Cristobalite	Dehydroxylation
5	S-17	0.481	201.65°-271.21°C	Muscovite	Dehydroxylation
		0.260	330.04°-369.56°C	Muscovite	Dehydroxylation
		0.376	572.59°-668.77°C	Quartz admixture of magnetite, olivine and spinel	Dehydroxylation
		0.853	1097.80°-1098.84°C	Cristobalite	Dehydroxylation
6	S-19	0.103	201.79°-255.28°C	Muscovite	Dehydroxylation
		0.084	342.07°-374.05°C	Muscovite	Dehydroxylation
		0.423	535.92°-687.13°C	Quartz admixture of magnetite, olivine and spinel	Dehydroxylation
		0.275	1131.54°-1163.87°C	Cristobalite	Dehydroxylation
7	S-21	0.936	214.49°-308.23°C	Muscovite	Dehydroxylation
		0.369	588.64°-643.18°C	Quartz admixture of magnetite, olivine and spinel	Dehydroxylation
		0.368	865.81°-901.53°C	Cristobalite	Dehydroxylation
		0.528	1029.90°-1103.74°C	Cristobalite	Dehydroxylation
8	S-23	0.264	198.11°-251.37°C	Muscovite	Dehydroxylation
		0.147	336.01°-372.75°C	Muscovite	Dehydroxylation
		0.288	533.20°-651.15°C	Quartz admixture of magnetite, olivine and spinel	Dehydroxylation

of Science and Technology) for providing financial support to carry out this work. First author would also like to thank, Mrs. Bharathi Murgod and Ganesh Kundaragi, University Science and Instrumentation Centre (USIC), Karnatak University, Dharwad and her technical assistant, Mr. Santosh Horatti for helping in handling instrumentation and providing FTIR data.

References

Annibale Mottana, Francesca Paolo Sassi, James, B. Thompson, Jr, Stephen Guggenheim. (2002). Micas: crystal chemistry and metamorphic petrology. *Reviews in mineralogy and geochemistry*. **46**, p. 41.

Bhaskar J.Saikia, Gopalakrishnarao parthasarathy (2010): Fourier transform infrared spectroscopic characterization of kaolinite from Assam and Meghalaya, northeastern India, *J. Mod., Phys*., **1,** 206-210.

Bhat, P.G.K., Raju, D. D., Ahmed, S., Venkatasubramanian, M., Anjanappa, B., Mohieddin, K. (1996). Specialized thematic mapping and geochemical surveys of Hundgund–Kushtagi–Hagari schist belt. *Record Geological Survey of India*, **129**, 71–77.

Dey, S. (2006). Petrology and geochemistry of selected clastic rocks of the kaladgi super group and basement Clospet Granites from Bagalkot District, Karnataka, India. *Unpublished Ph.D thesis*, Jadavpur university, Kolkata.

Dey, S. (2011). Sr and Pb isotope study of granitoids adjacent to the Hungund-Kushtagi schist belt, Dharwar Craton, Southern India. In: Varma, O.P., Sarkar, B.C., Varma, A.K., Mukherjee, M.K. & Singh,S (eds) New paradigms of exploration and sustainable mineral development: vision 2020. *Indian Geological Congress and Indian School of Mines, Dhanbad*, 733-741.

Dey, S., Rai, A. K., Chaki, A. (2009). Geochemistry of granitoids of Bilgi Area, northern part of Eastern Dharwar Craton, southern India-Example of transition TTGs derived from depleted source. *Journal of the Geological Society of India*.**73**, 854- 870.

Dey, S., Gajapathi Rao, R., Gorikhan, R.A., Veerabhaskar, D., Kumar, S & Kumar, M.K. (2003). Geochemistry and origin of northern Clospet Granite from Gudur-Guledagudda area, Baglkot district, Karnataka. *Journal of Geological Society of India*, **62**, 152-168.

Dey, S., Pandey, U.K., Rai, A.K., Chaki, A. (2012). Geochemical and Nd isotope constraints on petrogenesis of granitoids from NW part of eastern Dharwar Craton: Possible implications for late Archaen crustal accretion. *Journal of Asian earth Sciences*, **45**, 40-56.

Escalera, E. Antti, M. L., Oden M. (2012). Thermal treatment and phase formation in Kaolinite and illite based clays from tropical regions of Bolivia. *International Conference in Advanced Materials Research.*1-8.

Kapoor, B.S., Singh, H.B., Goswami, S.C., Abrol, I.P., Bhargava, G.P., Pal, D.K., (1981) Weathering of micaceous minerals in some salt-affected soils *Journal of the Indian Society of Soil Science*, **29**, 486-492.

Mahesh C. Swami, H. M. Jayasheela, Vishal C. Husure (2014). Infrared Spectra of Manganese ores from deogiri of sandur schist belt area Karnataka india, *International journal of research in advent technology,* **2** (2), 341-344

Marulardhaya C.Hiremath, A Sreenivasa and Ajaykumar N. Asode (2019) Infrared Spectroscopic Investigation of Sulfate And Other Associated Minerals of Hungund-Kushtagi Schist Belt With Special Reference to their modes of Vibration, *International Journal of Scientific & Technology Research*. **8** (12), pp 3013-3018

Ming Zhang, Ling wang, Shigeto Hirai, Simon A.T. Redfren and Ekhard K. H. Sanje (2005). Dehydroxylation and CO_2 incorporation in anhealed mica (sericite): An Infrared spectroscopic study. *American Mineralogist*, **90**, 173-180.

Mohan, R.M., Piercey, S.J., Kamber, B.S. Sriniasa sarma, D. (2013). Subduction related tectonic evolution of the Neoarchean Eastern Dharwar Craton, southern India: new geochemical and isotopic constraints. *Precambrian research*, **227**, 204-226.

Naqvi,S., Khan, R.M.K., Manikyamba,C., Ram Mohan,M., Kharma,T.C., (2006). Geochemistry of the Neoarchaean high-Mg basalts, boninites and adakites from the Kushtagi-Hungund greenstone belt of the Eastern Dharwar Craton (EDC); Implications for the tectonic setting. *Journal of Asian Earth Sciences*. **27**,25-44.

Rajendra M. Guruwadeyar, Ajaykumar N.Asode, A Sreenivasa. (2018). Thermal analysis of Chromite ores of Tagadur area, Nuggihalli Schist Belt, Karnataka, India. *Journal of Emerging Technologies and Innovative Research*, **5** (5), 658-663.

Stephen, Guggenheim, Yu-Hwa Cha, A.F., Koster Van Groos. (1987) Muscovite dehydroxylation; High-temperature studies. *American mineralogist*, **72**, 537-550

Taylor, A. S., Blumb, J. D., Lasaga, A. C., MacInnis, I.N. (2000) Kinetics of dissolution and Sr release during biotite and phlogopite weathering. *Geochimica et Cosmochimica Acta*, **64**, 1191-1208.